

## APSIDAL MOTION AND ABSOLUTE PARAMETERS OF 21 EARLY-TYPE SMC ECCENTRIC ECLIPSING BINARIES

P. ZASCHE<sup>1</sup> M. WOLF<sup>1</sup>

<sup>1</sup> Astronomical Institute, Charles University, Faculty of Mathematics and Physics, CZ-180 00, Praha 8,  
V Holešovičkách 2, Czech Republic

*Draft version February 14, 2019*

### ABSTRACT

We present the apsidal motion as well as the light curve analyses of 21 eccentric eclipsing binaries located in the Small Magellanic Cloud. Most of these systems have never been studied before, hence their orbital and physical properties as well as the apsidal motion parameters are given here for the first time. All the systems are of early spectral type, having the orbital periods up to 4 days. The apsidal motion periods were derived to be from 7.2 to 200 years (OGLE-SMC-ECL-2194 having the shortest apsidal period among known main sequence systems). The orbital eccentricities are usually rather mild (median of about 0.06), maximum eccentricity being 0.33. For the period analysis using the  $O-C$  diagrams of eclipse timings, in total 951 minima were derived from survey photometry as well as our new data. Moreover, 6 systems show some additional variation in their  $O-C$  diagrams, which should indicate the presence of hidden additional components in them. According to our analysis these third-body variations have periods from 6.9 to 22 years.

*Subject headings:* stars: binaries: eclipsing – stars: fundamental parameters – stars: early-type – Magellanic Clouds

### 1. INTRODUCTION

Eclipsing binaries still represent a most general method how to derive the basic stellar parameters of the individual components such as radii, masses, or luminosities (see e.g. Southworth 2012). With these quantities, we would be able to improve and calibrate the existing stellar evolution models (Torres et al. 2010, or Pols et al. 1997). Moreover, the eclipsing binaries (hereafter EBs) can also serve as suitable distance indicators, even for the close-by galaxies in the Local Group, see e.g. (Hilditch et al. 2005, or Vilardell et al. 2010).

A somewhat special group of EBs are those which have an eccentric orbit. For many such systems the detected apsidal motion (Claret & Giménez 2010) was analysed. Those systems were usually used for studying the internal structure constants and also to test the general relativity (Claret & Giménez 1993). Moreover, for several apsidal motion systems also an additional third body was detected, constituting even more dynamically interesting stellar system. For a compilation of such systems, see a catalogue by Bozkurt & Değirmenci (2007). Quite recently, a comprehensive catalogue of 623 galactic eccentric EBs was published by Kim et al. (2018), showing that about 5% of the systems with eccentric orbits have in general some third unseen components (only based on eclipse timing variations, ETV). Additionally, also the processes like orbital circularization (Zahn 2008), the distribution of period-eccentricity (Kiminki & Kobulnicky 2012, or Meibom & Mathieu 2005), or spin-orbit (mis)alignment can be studied thanks to these objects.

Concerning the same objects outside our Galaxy the situation is slightly different. Due to much lower luminosities, the data for extragalactic binaries only became available over the last two or three decades. This is mainly due to the large photometric surveys like MA-

CHO (Alcock et al. 1997, ranging the period 1992-2000), and OGLE (Udalski et al. 1992, OGLE II ranging 1997-2000, OGLE III 2001-2009, and OGLE IV 2010-2014) for both Magellanic Clouds. These surveys harvested a huge portion of eclipsing binaries, 6143 from the MA-CHO survey (Faccioli et al. 2007), and even 48605 from the OGLE survey (Pawlak et al. 2016). There are also many eccentric binaries with noticeable apsidal motion among these systems.

This was a subject of several studies during the last couple of years. We have already published a series of papers on apsidal motion in SMC and LMC: Zasche & Wolf (2013), Zasche et al. (2014), and Zasche et al. (2015). And besides that, the apsidal motion was studied by other authors, most recently (and also most comprehensively) by Hong et al. (2016) presenting altogether 90 systems with apsidal motion in SMC, and Hong et al. (2015) studying 27 SMC systems.

Our present study is a natural continuation of such an effort. In Section 2 we present the methods used for our analysis, while later in Section 3 we introduce some of our most interesting results, and finally in Section 4 we briefly discuss the findings and place them into a broader context.

### 2. METHODS OF ANALYSIS

The huge majority of the targets presented in this study belongs to three groups. A first group, consisting of five targets, contains objects which were already known to have eccentric orbits and were already studied before. However, we collected many new observations of these systems during the time span 2012-2018, hence we believe our analysis is better and more complete than the already published ones. Second group comprises such stars, which were only by-chance discoveries in these monitored fields of the stars from the first group and are also eccentric with apsidal motion. And

finally, eight systems were found scanning the OGLE III database systematically (star numbers 1-1000).

For all of these systems we tried to find all available data, i.e. photometry from the MACHO, OGLE, and our new data from the 1.54-m Danish telescope located on La Silla Observatory in Chile (hereafter DK154), equipped with the CCD camera, and *I* and *R* filters used (operated remotely from the Czech Republic). Standard reduction procedure was applied for these new images, using the bias and the flat fields to the CCD images. The comparison star was chosen to be close to the main target and with a similar spectral type. A custom-made aperture-photometry reduction software APHOT developed by M. Velen and P. Pravec, was used for the data reduction. The correction for differential extinction was not applied due to the close distance of the comparison star and the variable one and the resulting negligible difference in air mass and their similar spectral types. The other archival photometric data from OGLE and MACHO surveys were used in that way as they were already published earlier on the websites or databases devoted to these surveys.

For analysing the light-curve (hereafter LC) of these binaries, we used the programme PHOEBE v0.32 (Prša & Zwitter 2005), which is based on the Wilson-Devinney algorithm (Wilson & Devinney 1971 and Wilson 1979) and its later modifications. Because of missing spectroscopic data for most of the targets, there are several limitations and assumptions which need to be taken into account. At first, the mass ratios were kept fixed at  $q = 1.0$ . This approach is justified because all the systems are well-detached and the ellipsoidal variations outside of their minima are generally negligible. For such systems their photometric mass ratios can only hardly be derived, as quoted e.g. by Terrell & Wilson (2005). Only for these systems where some spectroscopic data and the radial velocities were published, we naturally used the mass ratio different from unity. We are aware of the fact that this assumption of  $q = 1.0$  is rather odd for some of the systems where the light curve shapes show quite different eclipse depths of both minima. Hence, we tried a test of using the method of deriving the photometric mass ratios presented by Graczyk (2003), which uses the assumption of both components located on the main sequence. For two systems from our sample which show significantly different eclipse depths (namely OGLE-SMC-ECL-0752 and OGLE-SMC-ECL-1214), this method of deriving the mass ratio from the luminosity ratio resulted in values of  $0.80 \pm 0.08$ , and  $0.61 \pm 0.06$  respectively. As one can see, both these numbers are away from unity, but still one can only speculate how these values are close to reality when having no information about the radial velocities (and also whether the main sequence assumption is appropriate or not). Having this alternative second LC fit, we also performed the subsequent analysis (deriving the times of minima and carried out the period analysis). The differences between this new solution and the original one with assumption  $q = 1.0$  are only marginal. The eccentricity and the apsidal motion period resulted in almost the same values (differing by less than 2%), well within their respective error bars.

The individual sources of information (MACHO, OGLE and our new Danish 1.54-m photometry) deal with different photometric filters, namely *B*, *R*, and *I*

TABLE 1  
HELIOCENTRIC TIMES OF MINIMA USED FOR ANALYSIS.

Star	HJD - 2400000	Error	Filter	Reference
OGLE-SMC-ECL-0397	49177.26427	0.00266	BR	MACHO
OGLE-SMC-ECL-0397	49178.03816	0.00207	BR	MACHO
OGLE-SMC-ECL-0397	49651.22368	0.00204	BR	MACHO
OGLE-SMC-ECL-0397	49651.99717	0.00238	BR	MACHO
OGLE-SMC-ECL-0397	49948.40351	0.00336	BR	MACHO
OGLE-SMC-ECL-0397	49949.17003	0.00059	BR	MACHO
...				

Note: Table is published in its entirety in the electronic supplement of the journal. A portion is shown here for guidance regarding its form and content.

(the OGLE *V* data were not used due to much better OGLE *I*, both in quality and quantity). Different filters were fitted separately in PHOEBE, hence also different eclipse depths and luminosity ratios were derived. The values given and discussed below in the Section 3 are only these ones obtained for the *I* filter because of the better quality and reliability. For the OGLE and MACHO data only the most deviating data points (more than 3 sigma away) were omitted.

Here we summarize the individual steps of the analysis:

- At the beginning a preliminary light curve analysis was carried out (Initial OGLE period used, only rough estimation of the eccentricity, etc.).
- Initial LC analysis was used to derive preliminary minima, which were then analyzed to roughly estimate the apsidal motion (with the assumption  $i = 90^\circ$ ) and to judge whether to include the system into our sample or not (see Section 4 below).
- Then, the eccentricity ( $e$ ), argument of periastron ( $\omega$ ) and apsidal motion rate ( $\dot{\omega}$ ) resulting from the apsidal motion analysis were used for the light curve analysis.
- A value of inclination ( $i$ ) from the LC analysis, was then used for the apsidal motion analysis.
- And finally, the resulting  $e$ ,  $\omega$ , and  $\dot{\omega}$  values from the apsidal motion analysis were kept fixed for the final LC analysis.

A so-called AFP (Automatic Fitting Procedure) method was routinely used for deriving the times of minima from the photometric surveys as well as our new data. It uses the whole light curve shape as a template to calculate precise time of mid-eclipse. The method itself is presented in Zasche et al. (2014). All the minima used for the analysis are given in Table 1.

### 3. THE RESULTS

As was already mentioned earlier in Section 2, a whole portion of systems is rather heterogeneous, hence it comprises also the stars already studied (which are rather brighter), as well as those ones never studied before, which are slightly fainter. In Table 2 we can see some basic information about the particular systems, where one can find besides the alternative designations of the particular star also its coordinates for precise identification. Besides that, the photometric indices as found in the various databases and surveys are given together

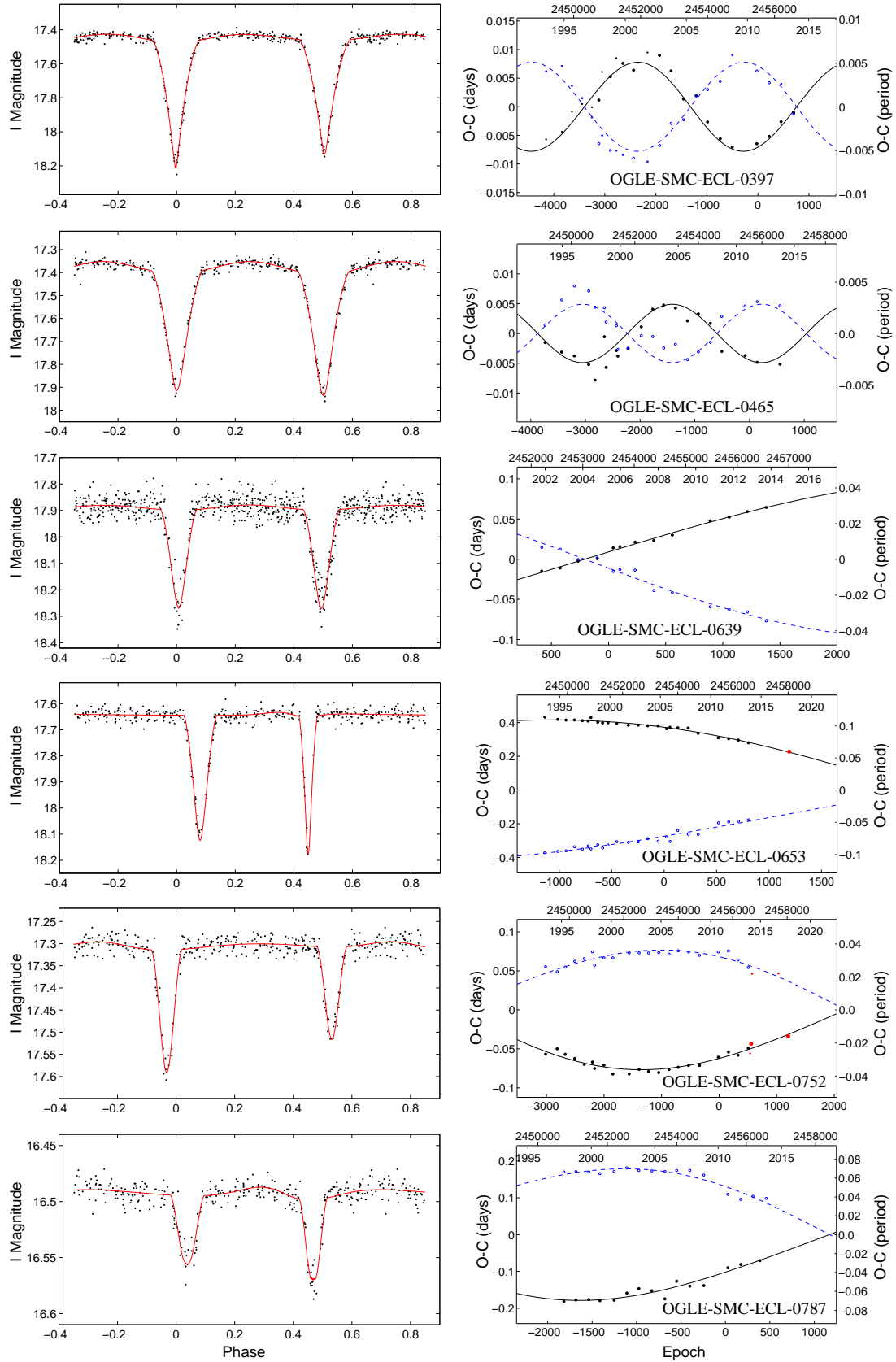


FIG. 1.— Plot of the light curves and  $O - C$  diagrams of the analysed systems. For the  $O - C$  diagrams the full dots stand for the primary minima (as well as the solid line), while the open circles represent the secondary minima (and the dashed curve). Red symbols stand for our new minima derived from photometry taken with Danish 1.54-m telescope in La Silla.

TABLE 2  
RELEVANT INFORMATION FOR THE ANALYSED SYSTEMS.

System name			RA	DEC	$V_{\text{max}}^A$	$(B - V)^B$	$(B - V)_0$	Sp.Type
OGLE III	OGLE II	MACHO			[mag]	[mag]	[mag]	
OGLE-SMC-ECL-0397	SMC-SC2 11454	213.15277.84	00:39:33.91	-73:18:55.8	17.279	-0.015	-0.294	
OGLE-SMC-ECL-0465	SMC-SC2 33379	213.15389.115	00:40:49.05	-73:27:54.8	17.253	0.389	-0.519	
OGLE-SMC-ECL-0639			00:43:16.20	-73:41:51.9	17.824	0.051	-0.163	
OGLE-SMC-ECL-0653	SMC-SC3 92887	213.15565.189	00:43:22.83	-73:05:11.2	17.516	-0.07	-0.113	
OGLE-SMC-ECL-0752	SMC-SC3 161183	212.15625.117	00:44:26.10	-72:56:48.0	17.200	-0.112	-0.251	
OGLE-SMC-ECL-0787	SMC-SC3 168989		00:44:43.83	-72:48:18.7	16.808	0.40	-0.069	
OGLE-SMC-ECL-0874	SMC-SC3 208420	212.15678.74	00:45:26.89	-73:10:05.1	16.328	0.10	-0.244	
OGLE-SMC-ECL-0929	SMC-SC4 47082	208.15685.160	00:45:44.60	-72:42:27.0	17.783	-0.14	-0.174	
OGLE-SMC-ECL-1214	SMC-SC4 121461	212.15792.439	00:47:24.66	-73:09:36.0	17.864	-0.284	-0.074	
OGLE-SMC-ECL-1370	SMC-SC4 160094	212.15847.154	00:48:10.16	-73:19:37.5	16.986	-0.020	-0.251	B2 <sup>C</sup>
OGLE-SMC-ECL-1393	SMC-SC4 175333	212.15850.358	00:48:15.35	-73:07:05.7	17.648	0.10	-0.256	B1 <sup>C</sup>
OGLE-SMC-ECL-1558	SMC-SC5 7078		00:49:02.31	-73:27:48.2	14.108	-0.12	-0.269	B2 <sup>C</sup>
OGLE-SMC-ECL-1634	SMC-SC5 123390	212.15908.2537	00:49:22.65	-73:03:43.2	16.023	0.05	-0.278	B0-5(II) <sup>D</sup>
OGLE-SMC-ECL-1874	SMC-SC5 185408	212.15962.211	00:50:24.53	-73:14:56.4	17.405	-0.031	-0.266	B1 <sup>C</sup>
OGLE-SMC-ECL-1985	SMC-SC5 225507	208.16025.300	00:50:49.11	-72:50:21.7	17.629	-0.034	-0.207	B2 <sup>C</sup>
OGLE-SMC-ECL-2112	SMC-SC5 266084		00:51:18.84	-73:14:01.8	17.180	0.09	-0.195	
OGLE-SMC-ECL-2152	SMC-SC5 265970	212.16076.59	00:51:28.10	-73:15:18.0	16.121	0.03	-0.230	B1 <sup>C</sup>
OGLE-SMC-ECL-2194	SMC-SC5 266131	212.16077.197	00:51:35.80	-73:12:45.2	17.071	0.056	-0.280	B1 <sup>C</sup>
OGLE-SMC-ECL-2385	SMC-SC6 67902	208.16084.193	00:52:12.12	-72:44:53.6	17.126	0.445	-0.611	
OGLE-SMC-ECL-2460	SMC-SC6 100626	212.16133.476	00:52:29.95	-73:16:51.6	18.526	0.103	-0.150	
OGLE-SMC-ECL-4923	SMC-SC10 41690		01:04:39.47	-72:49:49.8	15.952	-0.20	-0.283	

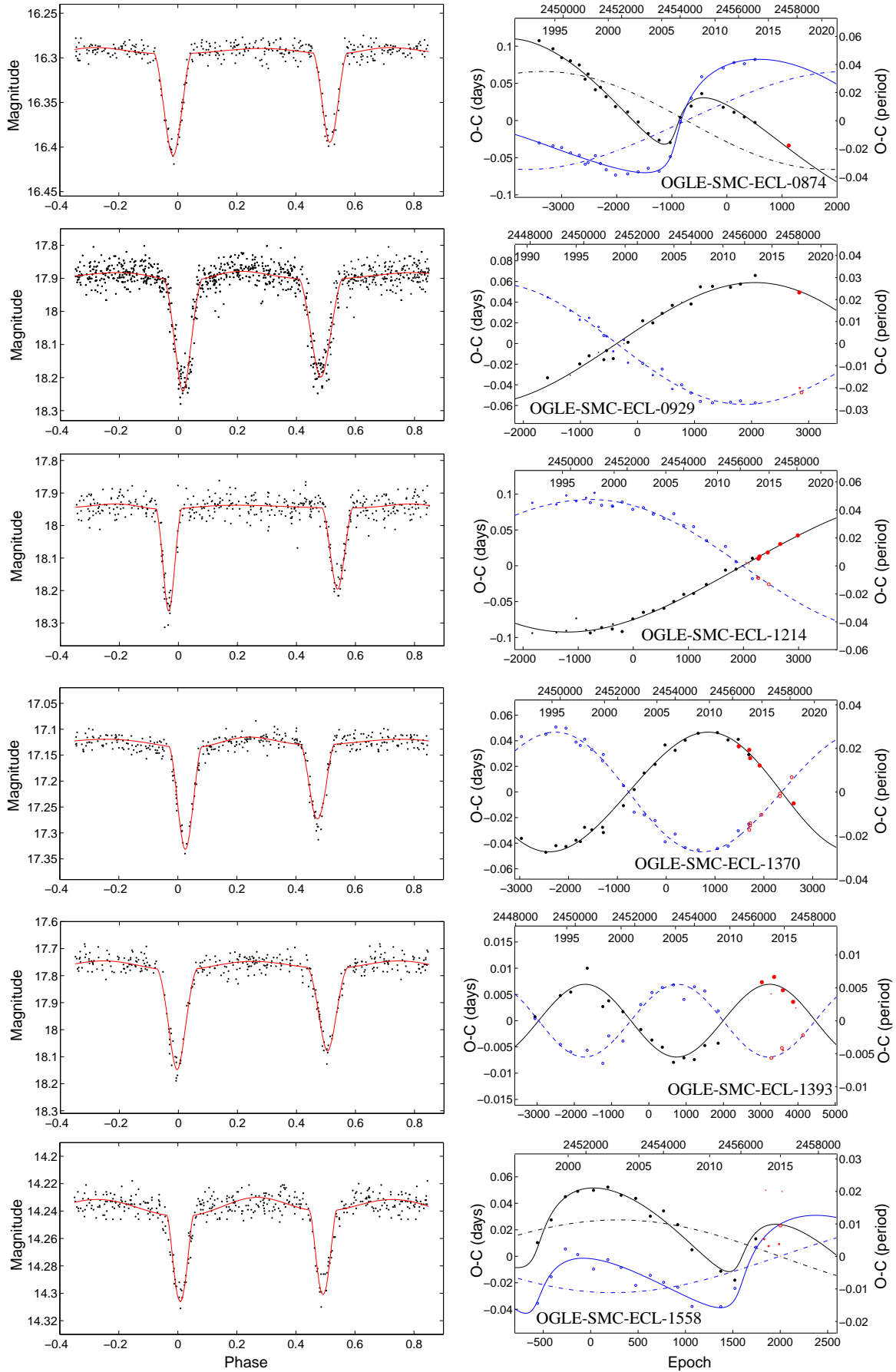
Note: [A] - Out-of-eclipse  $V$  magnitude based on OGLE database, see Pawlak et al. (2013); [B] - photometric index by Zaritsky et al. (2002) or Massey (2002); [C] - spectral type from North et al. (2010), and [D] - from Evans et al. (2004).

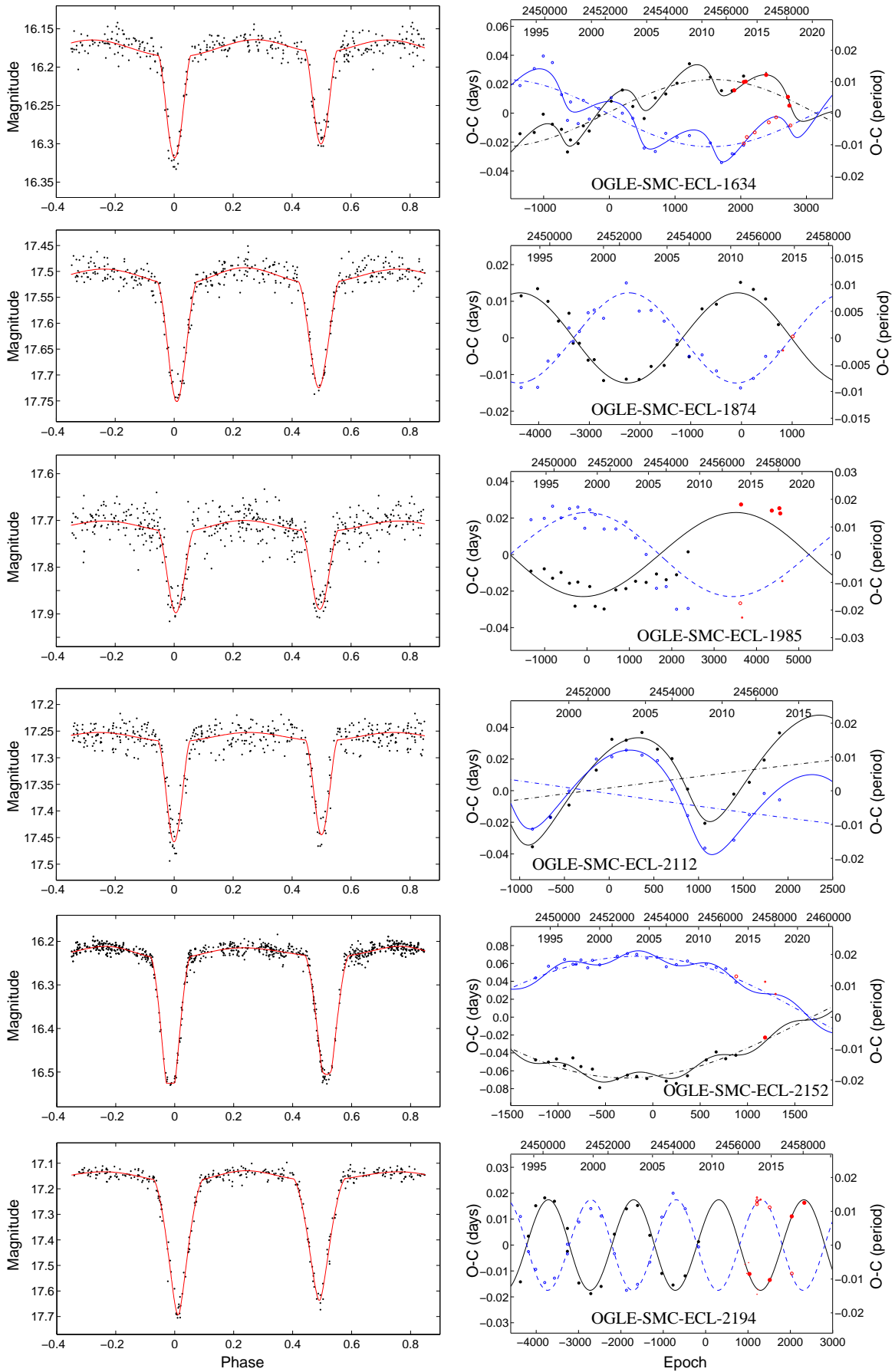
TABLE 3  
THE PARAMETERS OF THE LIGHT CURVE FITS AND THE APSIDAL MOTION.

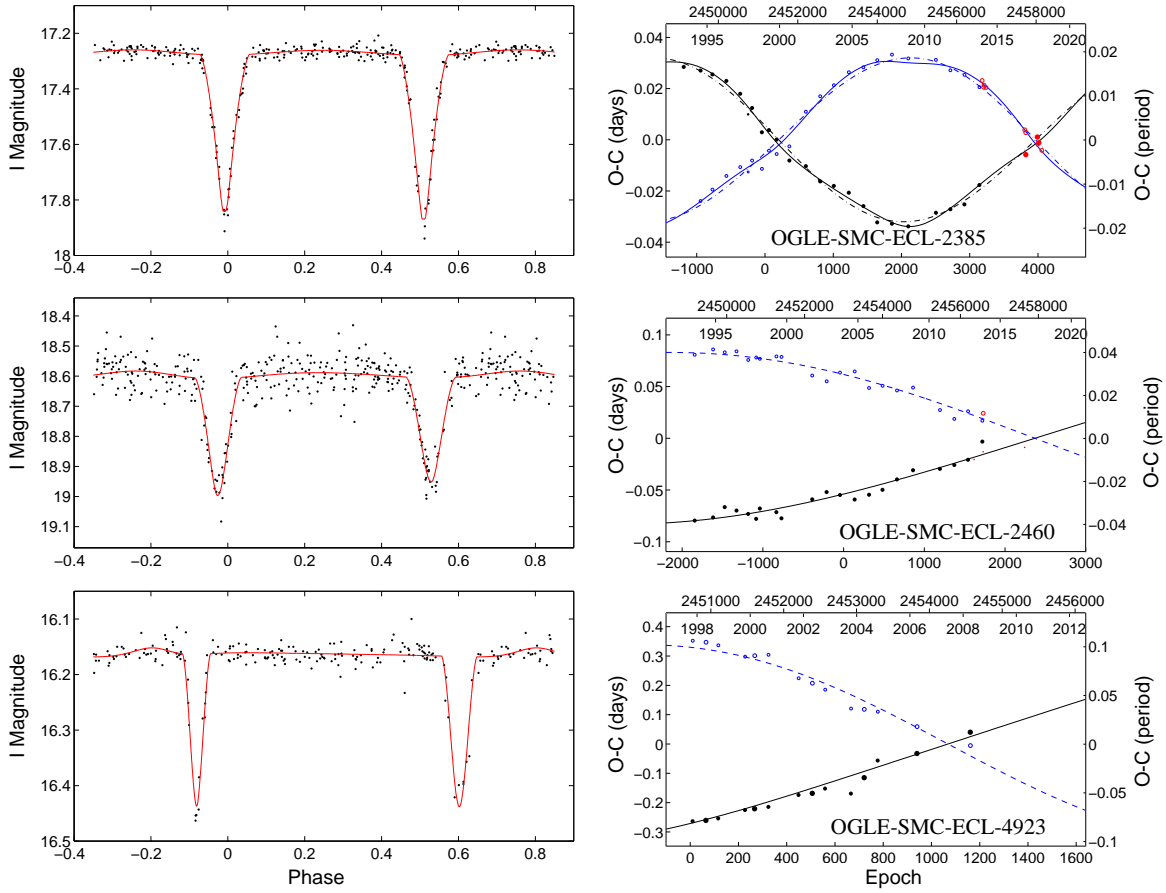
System	$i$ [deg]	$T_1$ [K]	$T_2$ [K]	$L_1$ [%]	$L_2$ [%]	$L_3$ [%]	$R_1/a$	$R_2/a$	$HJD_0$ [2400000+]	$P$ [d]	$e$	$\omega$ [deg]	$U$ [yr]
OGLE-SMC-ECL-0397	90.96 (0.98)	29000	28238 (370)	51.5 (1.9)	48.5 (1.7)	0.0	0.262 (2)	0.259 (2)	55503.3151 (14)	1.5239810 (12)	0.016 (4)	24.3 (0.8)	17.4 (0.9)
OGLE-SMC-ECL-0465	85.09 (1.22)	15000	15743 (305)	40.2 (1.4)	57.0 (3.2)	2.8 (3.0)	0.256 (5)	0.296 (4)	55610.2068 (9)	1.7208977 (8)	0.009 (2)	335.5 (0.9)	15.4 (0.7)
OGLE-SMC-ECL-0639	82.22 (0.75)	16000	17121 (1216)	42.0 (3.2)	57.8 (3.8)	0.2 (0.7)	0.193 (7)	0.217 (3)	53501.2182 (68)	2.2176130 (63)	0.140 (19)	95.8 (2.6)	77.5 (16.9)
OGLE-SMC-ECL-0653	86.58 (0.30)	13000	11973 (349)	60.3 (1.0)	37.8 (1.5)	1.8 (1.0)	0.154 (3)	0.133 (2)	53502.2863 (209)	3.8022773 (109)	0.333 (87)	216.8 (18.5)	170.1 (43.7)
OGLE-SMC-ECL-0752	79.59 (0.63)	24000	21353 (439)	56.1 (2.3)	40.9 (2.0)	3.0 (1.8)	0.187 (4)	0.172 (2)	55500.8284 (52)	2.1130468 (77)	0.114 (24)	31.4 (4.9)	78.0 (7.3)
OGLE-SMC-ECL-0787	82.38 (1.06)	10500	10590 (548)	6.0 (0.8)	20.9 (3.1)	73.1 (4.8)	0.116 (2)	0.235 (4)	55402.2604 (86)	2.5592298 (101)	0.217 (55)	48.8 (6.0)	71.6 (8.2)
OGLE-SMC-ECL-0874	80.16 (0.62)	25000	20483 (498)	29.4 (1.1)	13.1 (0.3)	57.5 (2.3)	0.219 (3)	0.177 (4)	55601.0605 (60)	1.8846380 (52)	0.109 (15)	294.2 (3.2)	56.7 (4.0)
OGLE-SMC-ECL-0929	79.43 (0.57)	17000	17630 (420)	48.3 (1.0)	51.7 (1.8)	0.0	0.229 (5)	0.231 (5)	52003.2937 (23)	2.1273835 (22)	0.087 (12)	104.1 (2.8)	54.2 (3.2)
OGLE-SMC-ECL-1214	82.44 (0.61)	21000	20757 (629)	68.5 (1.4)	31.5 (0.9)	0.0	0.188 (4)	0.131 (3)	52217.6935 (42)	1.9467130 (12)	0.148 (17)	29.9 (3.1)	63.4 (4.9)
OGLE-SMC-ECL-1370	76.53 (0.22)	25000	22437 (431)	57.2 (3.2)	36.1 (3.8)	6.7 (2.9)	0.217 (5)	0.191 (3)	53689.5886 (11)	1.6996138 (13)	0.086 (7)	134.2 (2.3)	29.1 (1.5)
OGLE-SMC-ECL-1393	81.09 (0.90)	21000	18211 (510)	68.0 (2.3)	32.0 (2.0)	0.0	0.257 (4)	0.190 (7)	52473.2811 (6)	1.2511244 (4)	0.017 (3)	305.1 (1.1)	16.9 (0.9)
OGLE-SMC-ECL-1558	71.06 (0.31)	26400	22643 (335)	40.9 (3.4)	27.0 (1.5)	32.1 (2.8)	0.223 (6)	0.209 (7)	52150.9320 (42)	2.4472722 (45)	0.035 (22)	166.4 (5.2)	46.4 (7.4)
OGLE-SMC-ECL-1634	77.90 (1.15)	28000	22920 (329)	77.1 (0.9)	12.6 (1.4)	10.3 (3.7)	0.248 (3)	0.129 (6)	52132.9208 (22)	2.1728736 (18)	0.034 (25)	91.8 (4.7)	37.8 (2.3)
OGLE-SMC-ECL-1874	75.98 (0.56)	21000	19545 (454)	60.1 (0.7)	39.9 (0.5)	0.0	0.253 (2)	0.214 (3)	55500.5525 (16)	1.4549890 (9)	0.027 (5)	187.7 (3.9)	17.1 (0.9)
OGLE-SMC-ECL-1985	75.04 (0.73)	20500	21089 (688)	60.7 (0.8)	39.3 (0.9)	0.0	0.244 (3)	0.195 (3)	51175.9685 (30)	1.5109147 (16)	0.048 (12)	2.7 (8.6)	29.2 (5.6)
OGLE-SMC-ECL-2112	82.28 (1.89)	18000	16971 (539)	32.3 (7.0)	26.5 (3.8)	41.2 (7.5)	0.194 (9)	0.182 (9)	52500.5798 (59)	2.1319415 (92)	0.059 (58)	92.5 (11.7)	190.2 (28.8)
OGLE-SMC-ECL-2152	90.81 (1.01)	23000	22413 (231)	69.9 (2.6)	21.1 (1.2)	9.0 (4.3)	0.265 (2)	0.149 (4)	53503.1812 (102)	3.4956503 (112)	0.061 (17)	9.3 (5.3)	7.2 (12.9)
OGLE-SMC-ECL-2194	83.61 (0.65)	26500	25280 (542)	59.8 (1.9)	40.2 (1.7)	0.0	0.285 (6)	0.243 (5)	55001.0438 (12)	1.3029425 (8)	0.042 (5)	126.3 (1.0)	7.2 (0.3)
OGLE-SMC-ECL-2385	92.02 (0.78)	20000	20010 (341)	44.9 (2.8)	50.8 (2.4)	4.3 (2.6)	0.198 (3)	0.209 (7)	51173.6235 (14)	1.7186416 (14)	0.058 (10)	260.3 (1.2)	35.4 (2.1)
OGLE-SMC-ECL-2460	81.66 (1.04)	15000	14825 (553)	54.8 (3.0)	45.2 (4.1)	0.0	0.218 (3)	0.201 (9)	53000.3362 (76)	2.0724939 (80)	0.121 (22)	43.1 (3.9)	85.7 (9.8)
OGLE-SMC-ECL-4923	82.36 (0.51)	26000	31350 (751)	43.4 (2.6)	56.6 (2.4)	0.0	0.138 (6)	0.141 (4)	50716.9851 (128)	3.3114695 (104)	0.312 (88)	24.2 (10.0)	53.0 (12.5)

TABLE 4  
THE PARAMETERS OF THE THIRD-BODY ORBITS FOR THE INDIVIDUAL SYSTEMS.

System	$A$ [days]	$\omega_3$ [deg]	$P_3$ [yr]	$T_0$ [HJD] [2400000+]	$e_3$	$f(m_3)$ [ $M_\odot$ ]	$P_3^2/P$ [yr]	$P^2/P_3^{5/3}$ [ $\times 10^{-5}$ ]
OGLE-SMC-ECL-0874	0.0497 (68)	342.0 (16.3)	21.4 (0.2)	69450 (225)	0.727 (28)	3.71 (56)	88453	0.12
OGLE-SMC-ECL-1558	0.0250 (49)	334.6 (21.3)	14.3 (0.9)	61228 (407)	0.652 (104)	0.75 (8)	30720	0.38
OGLE-SMC-ECL-1634	0.0110 (23)	207.1 (4.3)	6.9 (0.7)	58164 (112)	0.473 (52)	0.19 (2)	7937	1.01
OGLE-SMC-ECL-2112	0.0295 (30)	230.2 (24.0)	11.9 (0.1)	58979 (314)	0.406 (97)	1.06 (14)	24093	0.39
OGLE-SMC-ECL-2152	0.0057 (14)	254.6 (54.8)	7.5 (2.4)	56964 (661)	0.005 (5)	0.017 (2)	5888	2.28
OGLE-SMC-ECL-2385	0.0020 (10)	229.8 (48.2)	9.2 (1.5)	57975 (439)	0.184 (101)	0.0005 (1)	17844	0.39


 FIG. 2.— Plot of the light curves and  $O - C$  diagrams, continuation.

FIG. 3.— Plot of the light curves and  $O - C$  diagrams, continuation.


 FIG. 4.— Plot of the light curves and  $O - C$  diagrams, continuation.

with the dereddened value of  $(B - V)_0$ . These were calculated from the individual  $(B - V)$ , and  $(U - B)$  indices following the method published in Johnson (1958). However, in some cases this method yielded in rather unreliable results (this is the case for e.g. OGLE-SMC-ECL-0465, and OGLE-SMC-ECL-2385), hence even this spectral estimation cannot be used for deriving the primary temperature  $T_1$ . In most cases where some spectral classification was published earlier (by North et al. 2010, and Evans et al. 2004) our computed dereddened values of  $(B - V)_0$  resulted in quite reasonable values. The individual spectral types and their temperatures were assigned from the  $(B - V)_0$  values according to tables by Pecaut & Mamajek (2013).

For those systems where some spectroscopy was published the situation was a bit different. For several systems their radial velocity curves exist, and the resulting mass ratio  $q$  as published by North et al. (2010) was used for our modelling. Moreover, for one system (namely OGLE-SMC-ECL-1558) the spectral type classification together with the primary temperature value was also published (Evans et al. 2004), hence also this information was used. All the results of our fitting are given in Table 3 and Figures 1 to 4. In these light curve graphs we plotted only the data from shorter time interval when the change of  $\omega$  is only small (for better clarity not to plot the blurred phase light curve over the longer time interval due to precession of omega angle). In the Table 3 there are given the inclination  $i$ , fixed value of primary temperature  $T_1$ , computed temperature  $T_2$ , luminosity ratios

in  $I$  filter for all components, and relative radii of both stars – all of these as resulted from the PHOEBE fitting. Moreover, also the parameters from the apsidal motion analysis are given there, namely: linear ephemerides  $HJD_0$ , and  $P$  together with the eccentricity of the orbit  $e$ , argument of periastron  $\omega_0$  at a reference time of  $HJD_0$ , and also the apsidal period  $U$ .

As one can see, for a significant number of systems also an additional variation besides the apsidal motion was detected. We attributed this variation to some hypothetical additional third body in the system causing so-called light-time effect due to its orbital motion around a common barycenter. This method was described elsewhere (e.g. Irwin 1959, or Mayer 1990), and it is being almost routinely used nowadays for various surveys and satellite data, see e.g. Borkovits et al. (2016). For these systems, where an additional body was detected, their  $O - C$  diagrams after subtraction of the apsidal motion were plotted with the light-time effect fits, see Fig. 5. The parameters of these potential third-body orbits are given in Table 4, where the amplitude of variation is denoted as  $A$ , while  $\omega_3$  stands for the argument of periastron of the third orbit,  $T_0$  time of the periastron passage,  $P_3$  its period, and  $e_3$  its eccentricity, respectively. Mass function is  $f(m_3)$ , and the last two columns present the ratio of squared outer and inner periods, and the fraction  $P^2/P_3^{5/3}$ . Classical geometrical light-time effect has its amplitude proportional to  $\sim P_3^{2/3} \cdot f(m_3)^{1/3}$ , however, the dynamical perturbation is much more dominant in tight triples and its amplitude is proportional

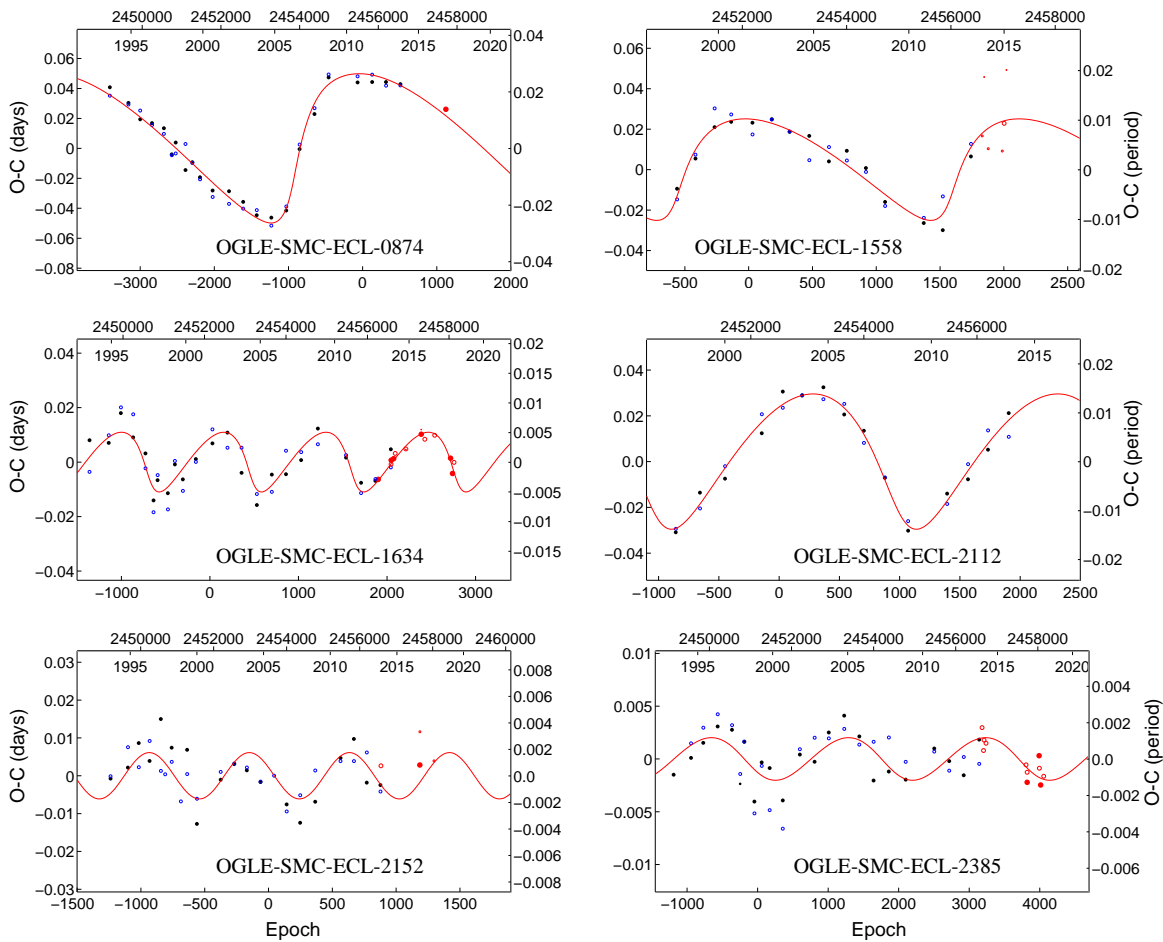


FIG. 5.— Plot of the  $O - C$  diagrams with the light-time effect fits (after subtraction of the apsidal motion).

to  $P^2/P_3 \cdot m_3/m_{1+2+3}$ , see e.g. Borkovits et al. 2016 for details. On the other hand, the slow precession of the orbits can possibly be detected only when the nodal period (Söderhjelm 1975) is adequately short, but its period is proportional to  $P_3^2/P$ . And as one can see, this ratio is too large for all of our studied systems. And finally, also the ratio of amplitudes for both contributions  $A_{dyn}/A_{LITE} \sim P^2/P_3^{5/3}$ , is adequately small for all of them.

Concerning the systems already studied in Hong et al. (2016), our presented fits seem to be better mainly due to the fact that we deal with larger data set, spanning longer period. Hence, our results should be more robust than the ones already published. The new data obtained with the Danish 1.54-m telescope were secured during the particular observing runs and present definitely more suitable photometry than the sparse OGLE photometric data (having typically only one data point per night).

We also computed the internal structure constants from the inferred apsidal motion. We calculated these values for seven systems from our sample which were also studied spectroscopically (by North et al. 2010), hence their masses are known precisely. The observed values were compared with the theoretical ones published by Claret (2005) as one can see in Table 5 and also Fig. 6. For the derivation of the theoretical values we used the same LMC metallicity as used by North et al. (2010), as well as the stellar ages derived from their analysis. The

relativistic contribution to the total apsidal motion rate is also given in Table 5, and is relatively small for all of the systems.

#### 4. DISCUSSION AND CONCLUSIONS

We have derived the preliminary apsidal motion and light curve parameters for 21 detached eclipsing binaries. Among these systems, several ones have already been studied before. However, we harvested also from other data sources, namely the spectroscopy (in contrast with the previous study by Hong et al. 2016), the long-term photometry for the better derivation of the apsidal motion (in contrast with the previous spectroscopic study by North et al. 2010), as well as our new precise photometry from the Danish 1.54-meter telescope.

The derived apsidal motion periods resulted in quite reasonable values of several decades (ranging from 7.2 to 200 years), and are usually well-constrained with the currently available set of photometric data. Thanks to the automatic surveys OGLE and MACHO, the time span is typically more than 20 years. The eccentricities are rather mild (mostly below 0.1, median of about 0.06).

We also detected altogether six systems showing besides the classical apsidal motion also some additional variation of their orbital periods. These six systems are shown in Fig. 5 together with their light-time effect fits, while the parameters of these fits are given in Table 4. One can see that the periods are adequately short, being still well-covered with the data. All of the systems



are definitely stable ones, according to the stability criteria as published earlier (see e.g. Mardling & Aarseth 2001, or Sterzik & Tokovinin 2002). In publications like Tokovinin (2004) there were presented several different empirical stability criteria with slightly different coefficients. However, all of our systems are located well below all of these stability limits in the  $P_3/P$  versus  $e_3$  diagram, hence our sample cannot be used for distinguishing between them. However, the more interesting dynamical effects of the third-body mechanics (Borkovits et al. 2016) are generally very small (see the last columns in Table 4 and Section 3 above). If we expect to find some dynamical influence of the third bodies on the eclipsing pairs (i.e. changing the inclination of the binary), it should be visible after several more decades or even a century of observations for two most promising systems (OGLE-SMC-ECL-1634 and OGLE-SMC-ECL-2152). For all of these systems a significant fraction of the third light was also detected during the LC analysis (see Table 3), which is an indirect evidence that our hypothesis is credible. We are aware of the fact that the whole analysis is based on assumption that the mass ratio of the eclipsing system is equal to 1.0. However, as we have tested for a few systems, the main results would be shifted when assuming different mass ratio, but the result about non/detection of the third light remains. Two other systems (namely OGLE-SMC-ECL-1985, and OGLE-SMC-ECL-4923) possibly also show additional third-body variations, but the orbital periods are probably longer ( $>20$  yr), hence we cannot do any reliable analysis yet.

The number of such potential third-body systems is increasing every year, even outside of our Galaxy, but our detected systems cannot be taken seriously as some comparative benchmark for statistics. This is mainly due to the fact that in our sample of stars we simply preferred these systems with more interesting variations in the  $O-C$  diagrams. Hence the number of such potential triples is apparently higher, than should be in real stellar population. However, the same apply also for the other apsidal motion systems in our sample, which were preferably selected only when having adequately short apsidal periods. In total, we have initially checked 35 obviously eccentric SMC systems, among which 21 were selected for the present publication due to their adequately short apsidal motion periods ( $U < 200$  yr).

And finally, quite remarkable situation arises when we compare the number of known system in and out of our own Galaxy. Kim et al. (2018) in their database lists in total 139 eccentric systems where the precession of omega angle is detectable within our Galaxy. However, thanks to recent papers on eccentric binaries in Magel-

lanic Clouds (such as Zasche et al. (2014), Zasche et al. (2015), Hong et al. (2015), Hong et al. (2016), or the present study) we can surely say that nowadays we know more such systems outside of our own Galaxy!

We are grateful to the anonymous referee for his/her fruitful comments and remarks, which greatly improved the whole manuscript. This work was supported by the grant MSMT INGO II LG15010. We also do thank the OGLE and MACHO teams for making all of the observations easily public available. We are also grateful

TABLE 5  
RELATIVISTIC APSIDAL MOTION AND OBSERVED INTERNAL  
STRUCTURE CONSTANT,  $\log k_{2,obs}$  FOR SEVEN SELECTED SYSTEMS.

System	$\dot{\omega}_{rel}$ [deg/cycle]	$\dot{\omega}_{rel}/\dot{\omega}$ [%]	$\log k_{2,obs}$
OGLE-SMC-ECL-1214	0.00186	6.15	-1.855
OGLE-SMC-ECL-1370	0.00243	4.23	-1.932
OGLE-SMC-ECL-1393	0.00204	2.80	-2.021
OGLE-SMC-ECL-1634	0.00221	3.90	-1.970
OGLE-SMC-ECL-1874	0.00235	2.80	-2.034
OGLE-SMC-ECL-2152	0.00154	3.25	-2.131
OGLE-SMC-ECL-2194	0.00299	1.68	-1.974

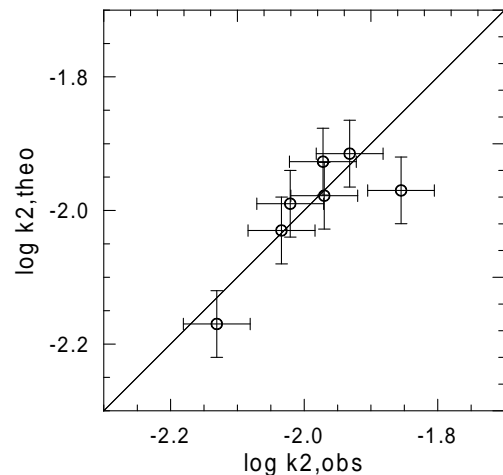


FIG. 6.— Internal structure constants, the observed ones compared with the theoretical ones.

to the ESO team at the La Silla Observatory for their help in maintaining and operating the Danish telescope. This research has made use of the SIMBAD and VIZIER databases, operated at CDS, Strasbourg, France and of NASA Astrophysics Data System Bibliographic Services.

#### REFERENCES

- Alcock, C., Allsman, R. A., Alves, D., et al. 1997, *ApJ*, 486, 697  
 Borkovits, T., Hajdu, T., Sztakovics, J., et al. 2016, *MNRAS*, 455, 4136  
 Bozkurt, Z., & Degirmenci, Ö. L. 2007, *MNRAS*, 379, 370  
 Claret, A. 2005, *A&A*, 440, 647  
 Claret, A., & Giménez, A. 1993, *A&A*, 277, 487  
 Claret, A., & Giménez, A. 2010, *A&A*, 519, A57  
 Evans, C. J., Howarth, I. D., Irwin, M. J., Burnley, A. W., & Harries, T. J. 2004, *MNRAS*, 353, 601  
 Faccioli, L., Alcock, C., Cook, K., et al. 2007, *AJ*, 134, 1963  
 Graczyk, D. 2003, *MNRAS*, 342, 1334  
 Hilditch, R. W., Howarth, I. D., & Harries, T. J. 2005, *MNRAS*, 357, 304  
 Hong, K., Kim, S.-L., Lee, J. W., et al. 2015, *AJ*, 150, 1  
 Hong, K., Lee, J. W., Kim, S.-L., Koo, J.-R., & Lee, C.-U. 2016, *MNRAS*, 460, 650  
 Irwin, J. B. 1959, *AJ*, 64, 149  
 Johnson, H. L. 1958, *Lowell Observatory Bulletin*, 4, 37  
 Kim, C.-H., Kreiner, J. M., Zakrzewski, B., et al. 2018, *ApJS*, 235, 41  
 Kiminki, D. C., & Koblunicky, H. A. 2012, *ApJ*, 751, 4  
 Mardling, R. A., & Aarseth, S. J. 2001, *MNRAS*, 321, 398  
 Massey, P. 2002, *ApJS*, 141, 81

- Mayer, P. 1990, BAICz, 41, 231  
Meibom, S., & Mathieu, R. D. 2005, ApJ, 620, 970  
North, P., Gauderon, R., Barblan, F., & Royer, F. 2010, A&A, 520, A74  
Pawlak, M., Graczyk, D., Soszyński, I., et al. 2013, AcA, 63, 323  
Pawlak, M., Soszyński, I., Udalski, A., et al. 2016, AcA, 66, 421  
Pecaut, M. J., & Mamajek, E. E. 2013, ApJS, 208, 9  
Pols, O. R., Tout, C. A., Schroder, K.-P., Eggleton, P. P., & Manners, J. 1997, MNRAS, 289, 869  
Prša, A., & Zwitter, T. 2005, ApJ, 628, 426  
Söderhjelm, S. 1975, A&A, 42, 229  
Southworth, J. 2012, Orbital Couples: Pas de Deux in the Solar System and the Milky Way, 51  
Sterzik, M. F., & Tokovinin, A. A. 2002, A&A, 384, 1030  
Terrell, D., & Wilson, R. E. 2005, Ap&SS, 296, 221  
Tokovinin, A. 2004, RMxAC, 21, 7  
Torres, G., Andersen, J., & Giménez, A. 2010, A&A Rev., 18, 67  
Udalski, A., Szymanski, M., Kaluzny, J., Kubiak, M., & Mateo, M. 1992, AcA, 42, 253  
Vilardell, F., Ribas, I., Jordi, C., Fitzpatrick, E. L., & Guinan, E. F. 2010, A&A, 509, A70  
Wilson, R. E., & Devinney, E. J. 1971, ApJ, 166, 605  
Wilson, R. E. 1979, ApJ, 234, 1054  
Zahn, J.-P. 2008, EAS Publications Series, 29, 67  
Zaritsky, D., Harris, J., Thompson, I. B., Grebel, E. K., & Massey, P. 2002, AJ, 123, 855  
Zasche, P., & Wolf, M. 2013, A&A, 558, A51  
Zasche, P., Wolf, M., Vraštil, J., et al. 2014, A&A, 572, A71  
Zasche, P., Wolf, M., Vraštil, J., & Pilarčik, L. 2015, AJ, 150, 183